Preprints of the 19th World Congress
The International Federation of Automatic Control
Cape Town, South Africa. August 24-29, 2014

Automated Transitions Between Walking and Running in Legged Robots

M. Shahbazi [*,**] **G.A.D. Lopes** [*] **R. Babuška** [*]

[*] *Delft Center for Systems and Control, Delft University of Technology, Mekelweg 2, 2628 CD Delft, The Netherlands.*
{*m.shahbaziaghbelagh; g.a.delgadolopes; r.babuska*}*@tudelft.nl*
[**] *Department of Mechatronics Engineering, Faculty of New Sciences and Technologies, University of Tehran, Iran.*

Abstract: This paper addresses the synthesis of controllers for walk-to-run transition (WRT) and run-to-walk transition (RWT) in legged robots with adjustable leg compliance. Inspired by human kinematics, we propose a detailed procedure for the WRT and RWT in an adjustable-stiffness spring and mass model, and derive control parameters that ensure effective gait transitions. The WRT is achieved by modulating the compliance of the leg in a piecewise constant way during the transition stride. In the RWT, in addition to the leg compliance, we modulate the touchdown angle of attack. The merits of the approach proposed are demonstrated via a simulation that incorporates the control of walking, followed by a transition to running with first increasing and then decreasing speed, and finally a transition back to walking.

Keywords: Walk-run transitions, Adjustable compliance, Controlled SLIP, Legged robots.

1. INTRODUCTION

Walking and running are the two gaits most commonly used by humans. In biomechanics, these two gaits are distinguished according to the patterns of the interleaved phases. While a flight phase is characteristic for running, walking entails a phase during which both legs are in contact with the ground at the same time (i.e., the double-stance phase). Although it is clear that humans prefer to transition from walking to running at a certain locomotion speed, there has been no unequivocal explanation as to why they change the gait (Prilutsky and Gregor, 2001). Biological observations (Hreljac et al., 2007) reveal that the transition stride does not resemble either of the two gaits, and that the transition is not a sudden event, but it is initiated during the transition stride and completed after an adjustment period. Hence, in order to study gait transitions, it is necessary to investigate the transient dynamics of the body.

In the control literature, the simulation and control of walk-run transitions has been rarely studied. The existing literature mainly focuses on identifying the overlap between stable limit cycles of walking and running. Initially, Geyer et al. (2006) claimed that there is a gap between the regions of stable walking and running limit cycles. However, Rummel et al. (2009) found an almost continuous morphing of gait patterns between walking and running. They showed that, in the case of a passive system, walking and running gaits can be produced at the same speed (at low and medium speeds). However, the authors did not address the transition process itself. More recently, Martinez and Carbajal (2011) detected a new gait pattern, namely 'hopping', that can connect a walking to a running limit cycle by using different angles of attack for each step. However, neither of these papers deals with adjustable compliance, something that is evidenced in the human morphology. Moreover, humans do not need to switch to an intermediate gait in the realization of walk-run transitions.

In this paper, we introduce a control methodology that realizes walk-to-run transition (WRT) and run-to-walk transition (RWT) along with the walking and running gaits in a unified framework. In Section 2 we explain why it is useful to exploit variable compliance in the leg and we formulate the underlying mathematical structure based on the spring-loaded inverted pendulum (SLIP) model. We also derive an approximate solution for the associated equations of motion that predicts the system behavior. This solution plays a crucial role in the synthesis of controllers that we design to automate the transitions. We limit the adjustment of the leg compliance to piecewise constant discrete changes. Next, in Section 3 we propose a method to control the transient behavior of the system in accelerated running on the basis of the solution derived previously. Section 4 is devoted to the main contribution of the paper, the realization of WRT and RWT. We suggest the start and end instant of the transient behavior in the transition stride and synthesize the sequence of control parameters that lead to the desired specifications. Section 5 presents numerical simulations and the corresponding results. In addition, we present a preliminary investigation on the relevance and feasibility of the proposed control methods in comparison to human data. Section 6 concludes the paper along with suggestions for future work.

2. DYNAMIC WALKING AND RUNNING

It is generally accepted that the simplest yet sufficiently descriptive mechanical model that captures the characteristics of the animals walking and running gaits is the SLIP

model. It was first introduced for running (Blickhan, 1989), and later extended to represent walking as well (Geyer et al., 2006). Most of the subsequent research have focused on identifying periodic limit cycles by searching the space of the possible system parameters. In the context of the running SLIP, thanks to the simplicity of the flight phase, the adjustment of the swing leg parameters (namely, angle of attack, stiffness and rest length) prior to touchdown has attracted some attention (Seyfarth and Geyer, 2002; Blum et al., 2007; Seyfarth et al., 2003; Ernst et al., 2009). The idea of varying stiffness has also been studied for the bipedal SLIP in (Visser et al., 2012) by using feedback linearization. Biological studies reveal that humans adjust their leg stiffness during each locomotion step to compensate for the heel strike impact, and also from one step to the next to change the gait frequency, see for example (Farley and Gonzalez, 1996). It is also evidenced in (Lipfert et al., 2012) that the simple SLIP model overestimates the amplitude of the leg length changes, suggesting that a more sophisticated model is required. This motivates investigating an adjustable-stiffness spring and mass model.

2.1 Adjustable-stiffness spring and mass model

The spring-loaded inverted pendulum with adjustable stiffness for the modeling of walking and running gaits is depicted in Fig. 1(a) and (b), respectively. The model consists of a point mass m bouncing in the sagittal plane (with gravitational acceleration g) on two telescopic, compliant legs. The legs are assumed mass-less and the leg rest length is denoted by l_0. The stiffness of the legs has a nominal constant part k_0 and a varying part k_i, $i \in \{1, 2\}$, which can be adjusted by the controller to an arbitrary bounded value.

A single step of the walking gait starts at the vertical leg orientation (VLO) in the *single-stance phase* (SSP), includes the touchdown event of the swing leg leading to the *double-stance phase* (DSP), followed by the liftoff of the rear leg and ends at VLO in the next SSP. Hence, the walking gait alternates between the SSPs and DSPs. The transition from the SSP to the DSP occurs when the fully stretched swing leg touches the ground. The angle of attack is denoted by α_{w}. The transition form the DSP to the SSP takes place if the rear leg is fully stretched. A single running step starts in the *flight phase* (FP), at the highest vertical position of the center of mass (CoM), called the apex. In this phase, no leg is in contact with the ground. The transition to the SSP takes place when the fully stretched leg touches the ground. The angle of attack is denoted α_{r}. The transition to the FP occurs after the liftoff when the leg reaches its rest length and the step ends at the next apex. Hence, during running the system alternates between the SSPs and FPs.

The equations of motion in the DSP are as follows:

$$\begin{bmatrix} m\ddot{x} \\ m\ddot{y} \end{bmatrix} = \begin{bmatrix} 0 \\ -mg \end{bmatrix} + \begin{bmatrix} \cos\theta_1 & \cos\theta_2 \\ \sin\theta_1 & \sin\theta_2 \end{bmatrix} \begin{bmatrix} f_{\mathrm{s}1} \\ f_{\mathrm{s}2} \end{bmatrix}, \qquad (1)$$

where θ_i measures the angle between the horizontal and the ith leg which has the positive sign in the counterclockwise direction, $f_{\mathrm{s}i}$ is the ith spring force being calculated from the following expression:

$$f_{\mathrm{s}i} = (k_0 + k_i)(l_0 - l_i),$$

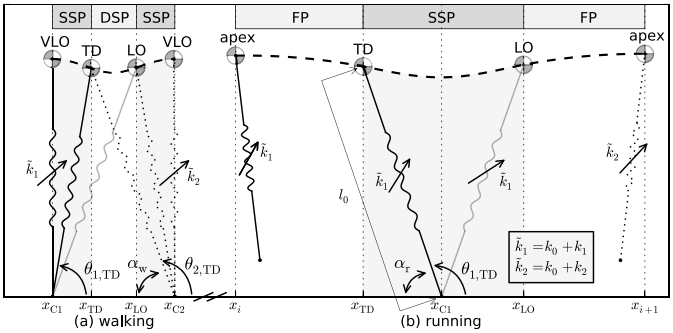

Fig. 1. Walking and running gaits performed using the adjustable stiffness spring-loaded inverted pendulum model. Subsequent single-stance phases are shaded.

and l_i is the instantaneous length of the ith leg. Note that if one sets $f_{\mathrm{s}1} = 0$ (or $f_{\mathrm{s}2} = 0$), then (1) represents the system dynamics in the SSP. Accordingly, for the FP both spring forces must be set to zero in (1). At the moment, a closed-form analytical solution for the differential equations (1) is not available. However, the control methods we propose in this paper rely on using the prediction of the system dynamics in the SSP. To fulfill this requirement and to avoid forward-in-time numerical simulations, we relax the accuracy and use an approximate analytical solution (Geyer et al., 2005) that has been proposed for the SLIP dynamics in the SSP.

2.2 Approximate map for the single-stance phase

Geyer et al. (2005) derived a simple analytical approximation, in terms of the elementary functions, for the SLIP dynamics in the SSP. While the approximation is quite accurate for symmetric trajectories, it introduces relatively large errors in asymmetric cases. Recently, Arslan et al. (2009) have improved the effectiveness of the original method by correcting the influence of the gravitational torque. In the rest of this section, after briefly reviewing this method, we describe how it can be modified to be used in the adjustable leg compliance case.

The equations of motion in the SSP, under the simplifying assumptions made in (Geyer et al., 2005), can be formulated in polar coordinates (r, θ) as:

$$\begin{aligned} \ddot{r} + \hat{\omega}_0^2 r &= f, \\ \dot{p} &= 0, \end{aligned} \qquad (2)$$

where $\hat{\omega}_0^2 = \omega_0^2 + 3\omega^2$, $f = -g + l_0\omega_0^2 + 4l_0\omega^2$, $\omega = p/(m{l_0}^2)$ and $\omega_0^2 = k/m$, with $p = mr^2\dot{\theta}$ being the angular momentum of mass m around the toe position assumed, at the moment, that is conserved during motion, hence can be substituted by the known angular momentum at the initial condition, $p_0 = mr_{\mathrm{ini}}^2\dot{\theta}_{\mathrm{ini}}$. Solving (2) and applying further simplifications yield the following expressions for the radial and angular motions in the SSP, by defining the instant of the initial condition as $t = 0$:

$$\begin{aligned} r(t) =& \frac{f}{\hat{\omega}_0^2} + \lambda_1 \sin\hat{\omega}_0 t + \lambda_2 \cos\hat{\omega}_0 t, \\ \theta(t) =& \frac{2g/l_0 + \omega_0^2 + \omega^2}{\hat{\omega}_0^2}\omega t \\ &+ \frac{2\omega}{l_0\hat{\omega}_0}(\lambda_1 \cos\hat{\omega}_0 t - \lambda_2 \sin\hat{\omega}_0 t) + \lambda_3, \end{aligned} \qquad (3)$$

where λ_1, λ_2 and λ_3 are constant values obtained from the initial conditions. Equation (3) is valid for any initial and final conditions within the SSP. Inspired by (Arslan et al., 2009), in order to improve the performance in case of asymmetric trajectories, we use the following equations to update the angular momentum:

$$\begin{aligned} \bar{r} &= \frac{f}{\hat{\omega}_0^2} + \frac{1}{\hat{\omega}_0 t_{\text{end}}}(\lambda_1 - \lambda_1 \cos\hat{\omega}_0 t_{\text{end}} + \lambda_2 \sin\hat{\omega}_0 t_{\text{end}}), \\ \bar{p} &= -\frac{t_{\text{end}}}{2} m g \bar{r}(\cos\theta_{\text{ini}} + \cos\theta_{\text{end}}), \\ p &= p_0 + \bar{p}. \end{aligned} \tag{4}$$

Now the updated angular momentum, p, replaces p_0 in the corresponding terms in (3).

This approximation assumes a constant stiffness for the leg. Having a chance to change the stiffness gives the opportunity to adjust the total energy of the system, which is necessary in order to achieve the desired locomotion properties. If we limit the variation of stiffness to discrete piecewise changes, then it is straightforward to adopt the above-mentioned approximation. The only required modification is to split the solution into n phases, if the leg compliance is intended to change for $(n-1)$ times between the initial and final positions. Of particular interest is the situation in which different constant stiffnesses are used for the spring compression (CP) and decompression (DCP) phases, $k = k_0 + k_{\text{c}}$ and $k = k_0 + k_{\text{dc}}$, respectively. Denoted by t_{b} the time for which $\dot{r}(t) = 0$ (i.e., the bottom position), we make a discrete change in the leg stiffness at $t = t_{\text{b}}$. Subsequently, $r(t_{\text{b}}), \theta(t_{\text{b}})$ and $\dot{\theta}(t_{\text{b}})$ define the new initial condition for the next phase solution. The resulting compliant leg with a multi-segment stiffness is a substantial part of the control methods we propose in the remaining of this paper.

Note that in the next sections we need to construct maps containing the FP dynamics as well. The derivation of a map between two arbitrary positions in the FP is straightforward due to the well-known ballistic motion. The reader can find the corresponding relations in (Geyer et al., 2005).

3. CONTROL OF ACCELERATED RUNNING

For the passive SLIP system, there exist stable limit cycles in walking and running that exhibit constant locomotion speeds (average per stride). Since we investigate walk-run transitions, we need to be able to accelerate the motion during particular intervals of time. In this paper we consider the accelerated motions when the robot is running. To do so, we synthesize a controller which makes use of (i) the multi-segment leg stiffness, and (ii) an adjustable leg touchdown angle of attack. The resulting deadbeat controller, which is based on the derived approximate solution (3), is used once per step, at apex, and computes the control inputs required to achieve the desired motion at the next apex, see Fig. 1(b). The state of the system at apex, z_i, can be defined by two variables [1]: the apex height, y_i, and the apex horizontal velocity, $\dot{x}_i$. Denoted by $\mathcal{Z} \in \mathbb{R}^2$ the set of possible apex states, we define the apex return map $H_{\text{r}} \colon \mathcal{Z} \to \mathcal{Z}$ such that:

$$z_{i+1} = H_{\text{r}}(z_i, u_i), \tag{5}$$

where $u_i = [\alpha_{\text{r}} \;\; k_{\text{c}} \;\; k_{\text{dc}}]^T$ is the vector of control parameters. The map H_{r} is the composition of the apex-to-touchdown map in the FP, the touchdown-to-bottom map with the leg compliance of $k = k_0 + k_{\text{c}}$ in the SSP, the bottom-to-liftoff map with the leg compliance of $k = k_0 + k_{\text{dc}}$ in the SSP, and the liftoff-to-apex map in the FP.

Biological evidence (Arampatzis et al., 1999) shows that during the SSP of running gait, humans constrain the maximum leg length change within a small domain, regardless of the locomotion speed that varies over an operational range. Using this experimental data it can be roughly estimated that the maximum leg retraction during the SSP is about 10% of the leg length, i.e.,

$$r_{\text{b}} = r(t_{\text{b}}) = 0.9 l_0. \tag{6}$$

This constraint can be added to (3) since it satisfies its prerequisite assumptions. Therefore, in order to derive the control parameters we need to solve the following equations together:

$$\begin{aligned} z_{i+1,\text{d}} - H_{\text{r}}(z_i, u_i) &= 0, \\ 0.9 l_0 - r(t_{\text{b}}(z_i, u_i)) &= 0. \end{aligned} \tag{7}$$

Since finding an analytical solution for (7) can be difficult, we solve this system of nonlinear implicit algebraic equations numerically. Note that efficient methods exist for quickly solving such a system of equations. Moreover, for a feasible range of the desired locomotion properties it always yields a solution since no constraints are imposed on the search space of k_{c} and k_{dc}. Solving (7) yields a vector of control parameters, u_i, that takes the system state at the current apex, z_i, to the desired state at the subsequent apex, $z_{i+1,\text{d}}$, in a single step of running gait.

4. WALK-RUN TRANSITIONS

In this section we propose a control methodology that realizes the walk-run transitions. In particular, we illustrate how the idea of using different stiffnesses for the spring CPs and DCPs helps us to synthesize controllers that automate practical transitions in a single step of locomotion. We hypothesize that the SSP in the WRT stride comprises of a CP and a DCP, while in the RWT stride it includes two CPs and one DCP. All the control calculations are on the basis of the derived approximate solution for the SSP in Section 2.2. Using (3) enables us to predict the system behavior without the need for forward-in-time simulations.

4.1 Control of walk-to-run transition

Fig. 2 depicts the proposed WRT-process schematically. Inspired by the real CoM movement trajectory observed for humans in (Segers et al., 2007), we assume that the WRT-process is triggered at the minimum height in the DSP (MHDS). The idea is to exploit different spring stiffnesses for the CP and DCP in the upcoming SSP in order to inject the energy required for a transitioning to the FP. The vector of control parameters is $u_i = [k_{\text{c}} \;\; k_{\text{dc}}]^T$. Here we have no control on α_{w} as it was established before the transition is triggered. The state of the system (for the purpose of control) at MHDS is defined as $z_{\text{m}} =$

[1] In order to describe the system state completely, we need to include the horizontal position of the mass in the state vector, but for the purpose of our control strategy this is not needed.

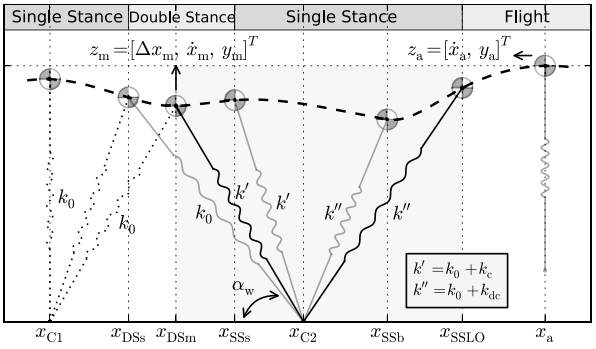

Fig. 2. Realization of WRT: Transition takes place in the shaded region.

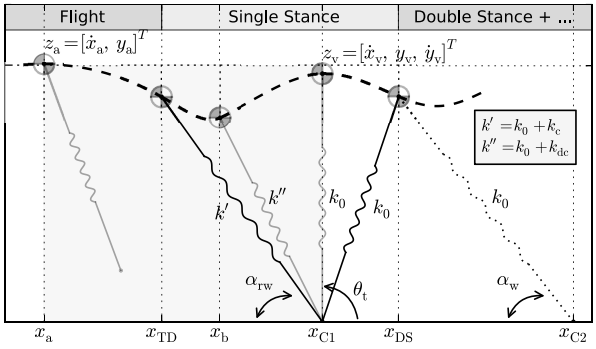

Fig. 3. Realization of RWT: Transition takes place in the shaded region.

$[\Delta x_m\ \dot{x}_m\ y_m]^T$, where $\Delta x_m = x_{C2} - x_m$. Similarly, we define the state of the system at apex as $z_a = [\dot{x}_a\ y_a]^T$.

According to Fig. 2, the map H_{wr} is built between the MHDS and the apex in the FP that immediately follows the SSP. It is important to note that although the MHDS belongs to a DSP, we ignore the influence of the rear leg and assume, at the moment, that the MHDS is a point in the upcoming SSP. The map H_{wr} is the composition of the following sub-maps: the MHDS-to-bottom map in the SSP (with the spring stiffness of $k' = k_0 + k_c$), the bottom-to-liftoff map in the SSP (with the spring stiffness of $k'' = k_0 + k_{dc}$), and the liftoff-to-apex map in the FP. Similarly to the procedure explained in Section 3, we formalize the problem as a system of implicit equations as follows:

$$z_{a,d} - H_{wr}(z_m, u_i) = 0, \tag{8}$$

with $z_{a,d} = [\dot{x}_{a,d}\ y_{a,d}]^T$ being the vector of the desired apex state. Solving (8) yields the required input vector u_i which realizes the WRT in a single step of locomotion.

The assumption that the MHDS belongs to the SSP is only made for the derivation of the control input, and does not take place in simulation. In the simulation, however, upon the control input u_i is calculated, the spring constant of the front leg, is updated but the simulated robot continues in the current DSP until the system naturally switches to the SSP. This is in accordance with what has been observed for human in (Segers et al., 2006) where in the transition stride the rear leg is walking and the front leg is running. However, one must adopt a control system that compensates for the effect of the rear leg force, which pushes the CoM forwards. Using physical insight and tuning in preliminary simulations, it was obtained that it is sufficient to adjust $z_{a,d}$ in advance. Accordingly, we reduce $\dot{x}_{a,d}$ by, roughly speaking, 50% and increase y_a by 50%. A quantitative demonstration for the proposed control strategy is given in Section 5.

4.2 Control of run-to-walk transition

In this section we propose a control strategy that realizes the RWT in a single step of locomotion. Fig. 3 illustrates the strategy schematically. The transition is triggered at the first apex for which $\dot{x}_a \leq \dot{x}_{rw}$, where $\dot{x}_{rw}$ is the preferred RWT speed. We assume that in the RWT the walking gait starts at VLO. Thereby the state of the system at VLO in the transition stride is defined by the walking gait specifications. To formalize the problem, denote by $z = [\Delta x\ \dot{x}\ y\ \dot{y}]^T$ the state of the system in the SSP, where $\Delta x = x_{C1} - x$. Accordingly, the desired state vector at VLO [2] (given by the walking limit cycle) is:

$$z_{v,d} = [0\ \dot{x}_{v,d}\ y_{v,d}\ 0]^T. \tag{9}$$

The control problem is to take z to $z_{v,d}$ in a single step of locomotion using the control input $u_i = [\alpha_{rw}\ k_c\ k_{dc}]^T$. Considering the system behavior in the SSP by looking at (3), we find that the radial motion, $r(t)$, has an oscillatory behavior, thereby the motion contains a sequence of peaks and valleys. Define the state of the system at a maximum radius as $z_t = [\Delta x_t\ \dot{x}_t\ y_t\ \dot{y}_t]^T$, where $\Delta x_t = x_{C1} - x_t$. In order to achieve $z_{v,d}$, it is necessary that the following property holds:

$$\theta_t = \theta(t_t(z_a, u_i)) = \frac{\pi}{2}, \tag{10}$$

i.e., the maximum radial motion occurs at VLO. Assuming (10) and taking into account that $\dot{y}_{TD} < 0$, it is necessary to have a local minimum in the system trajectory in the SSP before the VLO. The horizontal position of this point is denoted by x_b in Fig. 3. Taking into account the above-mentioned properties of the system, it follows that the spring in the SSP of the transition stride is first compressed until the CoM reaches x_b, and then switches to the DCP until the VLO. At this point, which is also the peak of the radial motion, it switches again to the CP. We make use of different stiffnesses for this *three-phase* movement in the SSP of the transition stride to conduct the transition process.

At the implementation side, we build the map H_{rw} between the apex state, z_a, and the state at VLO, z_v. Note again that given (10), z_v and z_t coincide. The map H_{rw} is the composition of three sub-maps: the apex-to-touchdown map in the FP, the touchdown-to-bottom map in the SSP with the leg compliance of $k' = k_0 + k_c$, and the bottom-to-VLO map in the SSP with the leg compliance of $k'' = k_0 + k_{dc}$. Similarly to the WRT, we formulate the problem as a system of implicit equations:

$$\begin{aligned} z_{v,d} - H_{rw}(z_a, u_i) &= 0, \\ \frac{\pi}{2} - \theta(t_t(z_a, u_i)) &= 0. \end{aligned} \tag{11}$$

Solving (11) yields the vector of control parameters, u_i, which realizes the RWT.

[2] We assume $\dot{y}_{v,d} = 0$ as demanded by the selected *symmetric* walking limit cycle.

5. SIMULATION RESULTS

In this section we demonstrate the effectiveness of the proposed methods for the realization of WRT and RWT quantitatively. In a simulation, see Fig. 4(top), the system starts to walk in a passive limit cycle with the average (per-stride) locomotion speed of $\bar{v}_{\rm w} = 1.17\,{\rm m/s}$ up to the time $t_{\rm wr} = 0.8\,{\rm s}$. At the first MHDS after $t_{\rm wr}$ the WRT controller calculates the control parameters that lead to the transition from walking to running, as proposed in Section 4.1. The transition takes place in one step and the robot is then instructed to run with the average (per-stride) positive acceleration of $\bar{a}_{\rm ar} = 0.766\,{\rm m/s^2}$, where the subscript 'ar' stands for *accelerated run*. At the time $t_{\rm cr} = 5.8\,{\rm s}$ the robot stops accelerating and keeps a constant locomotion speed of $\bar{v}_{\rm cr} = 5\,{\rm m/s}$ until $t_{\rm dr} = 6.3\,{\rm s}$. Next, a *decelerated run* with the negative average acceleration of $\bar{a}_{\rm dr} = -0.766\,{\rm m/s^2}$ continues until the first apex with the property of $\dot{x}_i \leq \dot{x}_{\rm rw} = 2\,{\rm m/s}$ is detected. At this instant the RWT controller, proposed in Section 4.2, is invoked and the control parameters are calculated accordingly. Consequently, the robot transitions to the similar walking limit cycle as the beginning. The simulation ends after a few strides in walking.

The top panel of Fig. 4 shows the desired and actual horizontal velocity (dashed and solid lines, respectively). The varying part of the legs stiffness are also plotted in dotted lines. The bottom panel of Fig. 4 shows the trajectory of the system together with the movement phase indicators are plotted. The WRT and RWT regions are highlighted in both subplots. A detailed view of these regions were already depicted in Figures 2 and 3. Table 1 reports the numerical values of the system parameters as well as the control parameters.

Discussion

As can be seen in the results, the WRT, the RWT and the accelerated running are realized effectively. In the following we explore some of the important features with respect to the numerical results obtained. In order to evaluate the feasibility of the results, we compare the calculated leg stiffness for the constant speed running using (5) with that of reported in (Arampatzis et al., 1999) for the human. The average estimated leg stiffness of several participants in their test for the speed of 5 m/s roughly equals to 31 kN/m which is quite similar to what can be read from Fig. 4 (top) for the similar speed ($k = k_0 + k_2 = 16.50 + 14.65 = 31.15\,{\rm kN/m}$). This match holds also for all other speeds that were reported. Moreover, the trajectory of the CoM during the WRT and RWT, see the highlighted parts in Fig. 4 (bottom) resemble those observed for a human in (Segers et al., 2007).

As depicted in Fig. 4, in order to accelerate the system in running, the controller commands a smaller stiffness for the CP than for the DCP. Together with the influence of the angle of attack, this shortens the decelerating part and prolongs the accelerating part in each SSP, making it possible for the system to increase the energy level, as demanded by the desired kinetic energy. Consequently, the locomotion speed and the step length increase. In contrast, for the decelerated running, the leg stiffness in the CP is larger than that of in the DCP, leading to smaller steps with reduced speeds.

Table 1. System and control parameters

System parameters:			
Body mass	m	80	kg
Gravity acceleration	g	9.81	m/s^2
Leg stiffness (constant part)	k_0	16.5	kN/m
Leg rest length	l_0	1	m
Walking limit cycle:			
Angle of attack	$\alpha_{\rm w}$	70	degree
$\dot{x}$ at starting VLO	$\dot{x}_{\rm v}$	1.11	m/s
y at starting VLO	$y_{\rm v}$	0.976	m
WRT (See Equation (8) and Fig. 2):			
$z_{\rm a,d} = \begin{bmatrix}\dot{x}_{\rm a,d} & y_{\rm a,d}\end{bmatrix}^T = \begin{bmatrix}0.6 & 1.5\end{bmatrix}^T$			
$z_{\rm m} = \begin{bmatrix}\Delta x_{\rm m} & \dot{x}_{\rm m} & y_{\rm m}\end{bmatrix}^T = \begin{bmatrix}0.2494 & 1.250 & 0.9220\end{bmatrix}^T$			
$u_i = [k_{\rm c} \;\; k_{\rm dc}]^T = \begin{bmatrix}-7.478 & 18.90\end{bmatrix}^T$			
RWT (See Equation (11) and Fig. 3):			
$z_{\rm v,d} = \begin{bmatrix}\Delta x_{\rm v,d} & \dot{x}_{\rm v,d} & y_{\rm v,d} & \dot{y}_{\rm v,d}\end{bmatrix}^T = \begin{bmatrix}0 & 1.11 & 0.976 & 0\end{bmatrix}^T$			
$z_{\rm a} = \begin{bmatrix}\dot{x}_{\rm a} & y_{\rm a}\end{bmatrix}^T = \begin{bmatrix}1.999 & 1.003\end{bmatrix}^T$			
$u_i = [\alpha_{\rm rw} \;\; k_{\rm c} \;\; k_{\rm dc}]^T = \begin{bmatrix}69.63 & 54.22 & -1.88\end{bmatrix}^T$			

It should be emphasized that the control methods proposed in this paper are based on the approximate solution of the SSP. Thereby, the approximation error is propagated throughout the simulation. This can affect the tracking performance or even cause a loss of stability. In particular in the RWT-process, since the system is intended to switch to a passive limit cycle with a very limited basin of attraction commonly attributed to passive limit cycles, the influence of the approximation error is noteworthy. Quantitatively, the system converges to $x_{\rm v} = [0 \;\; 0.9785 \;\; 1.052 \;\; -0.2485]^T$ instead of $z_{\rm v,d}$ given in Table 1, causing 5.2% error in $\dot{x}_{\rm v,d}$. Given this error, the system loses the stability of the subsequent walking limit cycle, although it can walk for a finite number of steps. This necessitates the existence of a regulator in the walking gait, which is out of the scope of the current work.

6. CONCLUSION

We have proposed a control synthesis method that enables an adjustable-stiffness spring and mass model to transition between walking and running gaits in a single step of locomotion. To realize the transition from walking to running the transition stride includes a single-stance phase with two distinct constant stiffnesses, changing in a piecewise discrete manner. For the run-to-walk transition the resulting stride contains three distinct constant stiffnesses. We have compared the simulation results with human data and concluded that there is a relevant agreement. In the future, we will explore the possibility of extending the findings to a more realistic robotic model incorporating segmented legs.

ACKNOWLEDGEMENTS

The first author gratefully acknowledges the support of the Government of the Islamic Republic of Iran, Ministry of Science, Research and Technology.

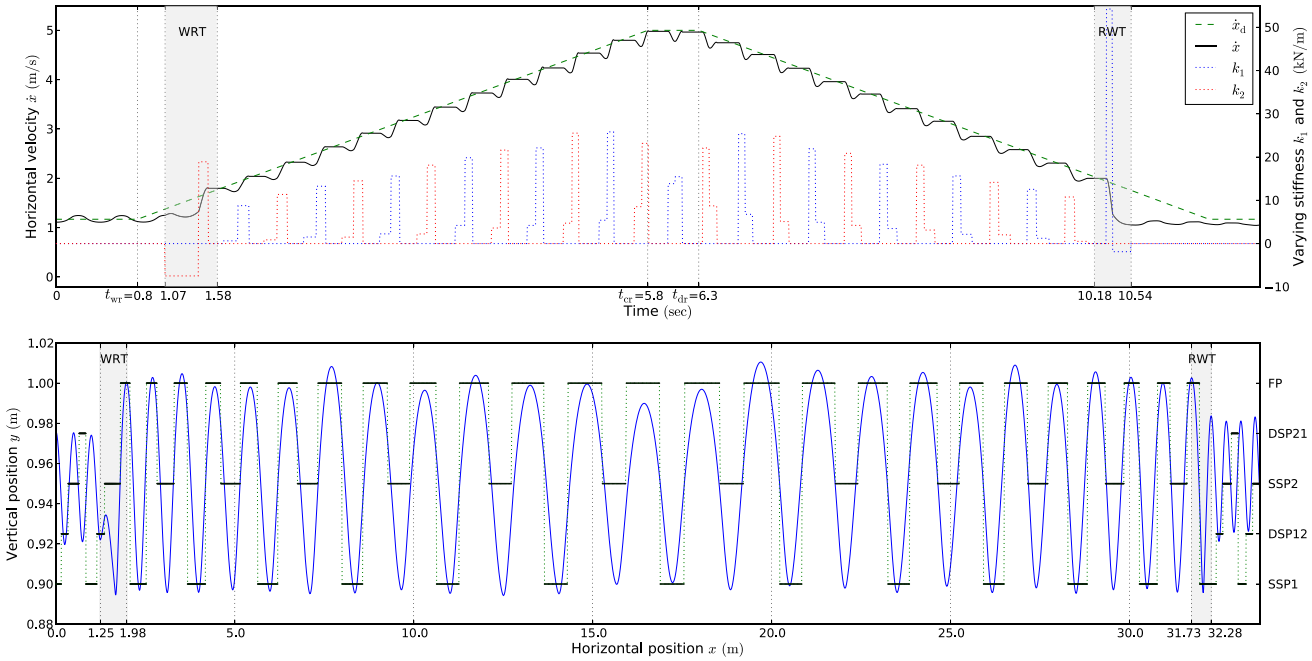

Fig. 4. The system starts in walking, switches to running with first increasing and then decreasing speed and finally transitions back to walking. Top: desired (dashed line) and actual (solid line) horizontal velocity along with the varying parts of the legs stiffness (dotted lines). Bottom: the corresponding CoM trajectory and phase indicators. In both panels, the WRT and RWT regions are highlighted.

REFERENCES

Arampatzis, A., Brüggemann, G.P., and Metzler, V. (1999). The effect of speed on leg stiffness and joint kinetics in human running. *Journal of biomechanics*, 32(12), 1349–1353.

Arslan, O., Saranli, U., and Morgul, O. (2009). An approximate stance map of the spring mass hopper with gravity correction for nonsymmetric locomotions. In *Robotics and Automation, 2009. ICRA'09. IEEE International Conference on*, 2388–2393. IEEE.

Blickhan, R. (1989). The spring-mass model for running and hopping. *J. biomechanics*, 22(11), 1217–1227.

Blum, Y., Rummel, J., and Seyfarth, A. (2007). Advanced swing leg control for stable locomotion. In *Autonome Mobile Systeme 2007*, 301–307. Springer.

Ernst, M., Geyer, H., and Blickhan, R. (2009). Spring-legged locomotion on uneven ground: a control approach to keep the running speed constant. In *International Conference on Climbing and Walking Robots (CLAWAR)*, 639–644. World Scientific.

Farley, C.T. and Gonzalez, O. (1996). Leg stiffness and stride frequency in human running. *Journal of biomechanics*, 29(2), 181–186.

Geyer, H., Seyfarth, A., and Blickhan, R. (2005). Spring-mass running: simple approximate solution and application to gait stability. *Journal of theoretical biology*, 232(3), 315–328.

Geyer, H., Seyfarth, A., and Blickhan, R. (2006). Compliant leg behaviour explains basic dynamics of walking and running. *Proceedings of the Royal Society B: Biological Sciences*, 273(1603), 2861–2867.

Hreljac, A., Imamura, R.T., Escamilla, R.F., and Edwards, W.B. (2007). When does a gait transition occur during human locomotion. *Journal of Sports Science and Medicine*, 6(1), 36–43.

Lipfert, S.W., Günther, M., Renjewski, D., Grimmer, S., and Seyfarth, A. (2012). A model-experiment comparison of system dynamics for human walking and running. *Journal of Theoretical Biology*, 292, 11–17.

Martinez, H.R. and Carbajal, J.P. (2011). From walking to running a natural transition in the slip model using the hopping gait. In *Robotics and Biomimetics (ROBIO), 2011 IEEE Int. Conference on*, 2163–2168. IEEE.

Prilutsky, B.I. and Gregor, R.J. (2001). Swing-and support-related muscle actions differentially trigger human walk–run and run–walk transitions. *Journal of Experimental Biology*, 204(13), 2277–2287.

Rummel, J., Blum, Y., and Seyfarth, A. (2009). From walking to running. In *Autonome Mobile Systeme 2009*, 89–96. Springer.

Segers, V., Aerts, P., Lenoir, M., and De Clercq, D. (2006). Spatiotemporal characteristics of the walk-to-run and run-to-walk transition when gradually changing speed. *Gait & posture*, 24(2), 247–254.

Segers, V., Lenoir, M., Aerts, P., and De Clercq, D. (2007). Kinematics of the transition between walking and running when gradually changing speed. *Gait & posture*, 26(3), 349–361.

Seyfarth, A. and Geyer, H. (2002). Natural control of spring-like runningoptimized self-stabilization. In *Proceedings of the Fifth International Conference on Climbing and Walking Robots. Professional Engineering Publishing Limited*, 81–85.

Seyfarth, A., Geyer, H., and Herr, H. (2003). Swing-leg retraction: a simple control model for stable running. *Journal of Experimental Biology*, 206(15), 2547–2555.

Visser, L., Stramigioli, S., and Carloni, R. (2012). Robust bipedal walking with variable leg stiffness. In *Biomedical Robotics and Biomechatronics (BioRob), 2012 4th IEEE RAS & EMBS Int. Conference on*, 1626–1631. IEEE.